Piezo1 mechanosensing regulates integrin-dependent chemotactic migration in human T cells

Chinky Shiu Chen Liu[1], Tithi Mandal[2], Parijat Biswas[3], Md. Asmaul Hoque[1,4], Purbita Bandopadhyay[1,4], Bishnu Prasad Sinha[1,4], Jafar Sarif[1,4], Ranit D'Rozario[1,4], Deepak Kumar Sinha[3], Bidisha Sinha[2], Dipyaman Ganguly[1]*

[1]IICB-Translational Research Unit of Excellence, CSIR-Indian Institute of Chemical Biology, Kolkata, India.

[2]Department of Biological Sciences, Indian Institute of Science Education and Research, Kolkata, India.

[3] Department of Biological Sciences, Indian Association for Cultivation of Science, Kolkata, India.

[4]Academy of Scientific and Innovative Research, Ghaziabad, India.

Correspondence: dipyaman@iicb.res.in

Running title: Piezo1 mechanosensing in human T cell chemotaxis

Keywords: Human T cells, Piezo1, Mechanosensing, Migration, Chemokine, Chemotaxis, Focal adhesion kinase, LFA-1, F-actin, Confocal Microscopy, Interference Reflection Microscopy

ABSTRACT

T cells are crucial for efficient antigen-specific immune responses and thus their migration within the body, to inflamed tissues from circulating blood or to secondary lymphoid organs, play a very critical role. T cell extravasation in inflamed tissues depends on chemotactic cues and interaction between endothelial adhesion molecules and cellular integrins. A migrating T cell is expected to sense diverse external and membrane-intrinsic mechano-physical cues, but molecular mechanisms of such mechanosensing in cell migration are not established. We explored if the professional mechanosensor Piezo1 play any role during integrin-dependent chemotaxis of human T cells. We found that deficiency of Piezo1 in human T cells interfered with integrin-dependent cellular motility. Piezo1 recruitment at the leading edge of moving T cells follows focal adhesion formation and local increase in membrane tension on chemokine receptor activation. Piezo1 activation constitutes a membrane-intrinsic component of the 'outside-in' signaling in human T cells, migrating in response to chemokines, that mediates integrin recruitment to the leading edge.

INTRODUCTION

Efficient T cell migration from blood circulation to secondary lymphoid organs and inflamed tissue is paramount for optimal tissue antigen sampling and effector functions during adaptive immune response (1-4). The process is dependent on chemotactic cues, interaction between endothelial adhesion molecules and T cell integrins, and an intricate acto-myosin dynamics (5). Generation of mechanical force is critical to propel migrating cells (6-9). Mechanosensing of the substrate and increase in cellular membrane tension is also intuitively apparent in a migrating T cell, although mechanistic details are not explored to a great extent.

Piezo1 and Piezo2 ion channels are evolutionarily conserved professional mechanosensors that can sense increase in membrane tension mostly independent of other protein-protein interactions (10-12). Mechanosensing by Piezo1 has been demonstrated to play critical role in diverse patho-physiologic contexts given its wide tissue expression including the immunocellular compartment (13-21). We previously identified crucial role of this specialized mechanotransducer in optimal TCR triggering (14, 19). The immunocellular expression of Piezo1 thus makes it a strong candidate for mechanosensing at the plasma membrane to regulate motility of immune cells. Piezo1 shows differential involvement if cellular migration depending on context (22- 28). Previous studies point to the possibility of a role of Piezo1 in confinement sensing and integrin activation in moving cells, while it deters integrin-independent cell motility, usually referred to as amoeboid movement (29, 30).

Here we aimed at exploring if Piezo1 mechanosensing plays any role during integrin-dependent chemotactic migration of human T cell migration, a patho-physiologically critical event in an ongoing immune response as well as in the steady-state. We found that deficiency of Piezo1 expression in human $CD4^+$ T cells as well as Jurkat T cells interfered with efficient integrin-dependent cellular motility in response to a chemotactic cue. We also found that Piezo1 activation constitutes a hitherto unknown membrane-intrinsic component of the 'outside-in' signaling in human T cells in response to chemokine receptor activation, that follows activation of focal adhesion kinase leading to local increase in membrane tension and mediates local recruitment of integrin molecules at the leading edge of the moving human T cells.

METHODS

siRNA-mediated Piezo1 knockdown

64 Human $CD4^+$ T lymphocytes were isolated from peripheral blood of healthy donors through
65 magnetic immunoselection. Cells were nucleofected with control EGFP or Piezo1 siRNA using Lonza
66 4D nucleofector. Knockdown was checked 72 hours post-nucleofection by quantitative PCR of Piezo1
67 and Piezo2 (Supplementary Figure 1A). For 2D motility assay, cells were co-nucleofected with Lonza
68 pmax-GFP plasmid and Piezo1 siRNA and motility difference between GFP^+ and GFP^+ cells were
69 assessed. Details of methodology are available as supplemental information.

70 **Cell motility assays**

71 2D non-directional motility was performed on ICAM1-coated dishes in presence of recombinant
72 human CCL19. 3D chemotaxis was performed using ICAM1-coated 5µm transwell inserts across
73 CCL19 and SDF1α gradients for $CD4^+$ T lymphocytes and Jurkat T cells, respectively. 2D tracking
74 analysis was performed using Fiji. Details of methodology are available as supplemental information.

75 **Membrane tension measurements**

76 Membrane tension of Piezo1-GFP expressing Jurkat cells was measured using non-invasive
77 interference reflection microscopy on fibronectin coated dishes upon addition of SDF1α. Analysis
78 was performed using MATLAB. Details of methodology for experiments and analyses are available as
79 supplemental information.

80 **Confocal imaging**

81 Fixed confocal imaging for Piezo1, pFAK, Akt, pAkt, LFA-1 and actin polarity in response to
82 chemokine stimulation was performed using Zeiss LSM confocal setup. Live cell imaging of Piezo1
83 mCherry and/or actin-GFP Jurkat T cells in the presence of SDF1α was performed using the same.
84 Polarity analysis was done on Fiji. Details of methodology for experiments and analyses are available
85 as supplemental information.

86

87 **RESULTS**

88 **Piezo1 deficiency abrogates integrin-dependent chemotactic motility in human T cells**

89 We first assessed the role of Piezo1 on integrin-dependent non-directional motility of primary
90 human $CD4^+$ T cells. We used GFP plasmid and Piezo1 siRNA co-transfected cells to facilitate
91 distinction between potentially transfected and nontransfected cells during cell tracking. We
92 compared the motility of GFP^+ T cells (presuming the transfection efficiency would lead to co-
93 transfection of siRNA) with the GFP^- T cells in the same culture. This was confirmed by flow

94 cytometric assessment of Piezo1 protein content on the T cell surface as well as the whole T cells
95 (Supplemental figures 1B, C). Piezo1 deficiency in T cells (potentially GFP^+) significantly hindered
96 their migration in response to CCL19 in terms of its mean-squared displacement (MSD, Figure 1A-C).
97 Representative cell tracks of Piezo1 deficient (GFP^+) and control (GFP^-) are shown in Figure 1B and
98 Supplementary Figure 1D.

99 ICAM1-coated transwell chemotaxis assay of human $CD4^+$ T lymphocytes and Jurkat T cells also
100 showed significant reduction in migration upon siRNA-mediated Piezo1 knockdown, in response to
101 CCL19 and SDF1α gradients, respectively (Figure. 1D, E). Piezo1 inhibition with GsMTx4 also led to
102 significant impairment of transwell chemotaxis (Supplementary figure 1E).

103

104 **Redistribution of Piezo1 toward the leading edge of migrating T cells in response to chemotactic**
105 **cue**

106 Cell polarity is a crucial aspect of directional cell motility in response to chemokines. $CD4^+$ T cells
107 seeded on ICAM-1 bed showed striking polarity in Piezo1 distribution, upon stimulation with CCL19
108 for 15 minutes (Figure 1F, G; Supplemental video 1). Piezo1 m-Cherry expressing Jurkat T cells also
109 showed striking leading edge polarity in the presence of SDF1α under ICAM1 adhesion (Figure 1H,
110 Supplemental Video 2). In Figure 1I, particle image velocimetry (PIV) analysis of a single
111 representative Jurkat cell has been shown to display the dynamically polarized Piezo1 fluorescence
112 upon SDF1α treatment with time, as opposed to rather uniformly distributed Piezo1 signals in a
113 representative untreated cell.

114

115 **Piezo1 redistribution in migrating T cells follow increased membrane tension in the leading edge**

116 Given its function, Piezo1 mechanosensors may play a role in sensing mechanical cues in a moving T
117 cell. We utilized the non-invasive technique of interference reflection microscopy or IRM for
118 studying potential redistribution of membrane tension following chemokine stimulation (31, 32).
119 IRM allows computation of tension magnitude from local temporal membrane fluctuations (Figure.
120 2A and detailed Methods in Supplementary Information). After baseline imaging, Piezo1-GFP
121 expressing Jurkat cells were subjected to sequential fluorescence and IRM imaging post SDF1α
122 addition which was followed over time. Chemokine administration to Jurkat T cells led to a decrease
123 in temporal fluctuations and an increase in membrane tension when computed for the whole
124 cellular contour (Figure 2B). The increase in membrane tension was registered within few minutes

125 after chemokine addition and gradually declined over time (Figure 2C). Distribution of tension and
126 fluctuation-amplitude in cells was also affected by the action of chemokine (Supplemental figure 2A)
127 which was accompanied by increase in the membrane's degree of confinement and the effective
128 viscosity experienced (Supplemental figure 2C & D). Moreover, the tension maps showed that the
129 lamellipodial structures towards the leading edges of the cells had higher tension magnitudes (Figure
130 2D, Supplemental figure 2B). These high-tension edges are usually further emphasized at later time-
131 points.

132 Finally, we explored if local membrane tension increase was linked to Piezo1 redistribution in the
133 chemokine-experienced T cells. Of note here, during acquisition, there was typically a time delay of 1
134 minute between measurement of tension and Piezo1-GFP fluorescence. As expected, average
135 tension peaked within the first few minutes of chemokine addition, followed by partial decline
136 (Figure 2E) as seen for the whole cell. Pixel count of Piezo1-GFP intensity showed a similar pattern,
137 albeit, at a delayed time, following the tension kinetics. In order to account for the delayed kinetics
138 of tension magnitude and Piezo1-GFP pixel count, we performed a correlation between normalised
139 Piezo1 pixel intensity at a particular time-frame, with normalised tension magnitude at the
140 preceding time frame. We observed significant positive correlation between the two parameters
141 (Figure 2F, G). Thus, IRM-coupled fluorescence microscopy revealed an increase in local membrane
142 tension in the leading edge of the moving T cells in response to chemokine receptor activation that
143 was associated with Piezo1 redistribution to the leading edges of the cells.

144

145 **Focal adhesion following chemokine receptor activation does not depend on Piezo1**

146 Focal adhesion formation induced by chemokine signaling is a critical step in cellular migration (33,
147 34). Anchoring of the local sub-membrane cytoskeleton with the extracellular substrate at sites of
148 focal adhesion complexes increases local membrane tension, which triggers membrane recruitment
149 and activation of integrins, through a mechanism of 'outside-in' signalling. This is followed by
150 integrin-dependent 'inside-out' signaling) driven primarily by phosphoinositide 3-kinase (PI3K)-Akt-
151 Rho-GTPase-actin polymerization pathway (35-38). Propelling forces generated by myosin-based
152 contractions and consequent F-actin retrograde flow allow the cells to move alone chemokine
153 gradients (6,7).

154 While phosphorylated FAK (pFAK) showed striking polarity upon CCL19 stimulation on ICAM-1 beds
155 (Figure 3A, B, Supplementary video 3), Piezo1 knockdown did not have any effect on pFAK polarity
156 under the same conditions (Figure 3C, D). Thus, focal adhesion formation following chemokine

157 receptor activation was not dependent on Piezo1. FAK activation recruits adapters like paxillin and
158 vinculin connecting the cortical cytoskeleton to the membrane and the extracellular matrix, thereby
159 increasing local membrane tension (33). Inhibition of FAK activation completely abrogated Piezo1
160 redistribution to the leading edge, hence the polarity (Figure 3E, F). This indicated that
161 mechanistically, FAK activation event precedes Piezo1 redistribution to the leading edge of the
162 migrating human $CD4^+$ T cells.

163 **Membrane recruitment of LFA1 on chemokine receptor activation disrupts with Piezo1 deficiency**

164 Integrin recruitment to the leading edge occurs downstream of FAK activation and local F-actin
165 polymerization. As expected, CCL19 stimulation led to LFA1 recruitment to the leading edge and,
166 Piezo1 and LFA1 exhibited significant colocalization upon CCL19 stimulation on ICAM1 bed (Figure
167 3G-I; Supplemental video 4). Piezo1 downregulation abrogated LFA-1 polarity (Figure 3J, K;
168 Supplemental videos 5, 6). Thus, role of Piezo1 in chemotactic migration of T cells was downstream
169 of FAK assembly in response to chemokine receptor signaling, but preceded integrins recruitment.
170 These data together point to a mechanism whereby local increase in membrane tension leading
171 from FAK activation and assembly drives Piezo1 activation, which in turn is linked to LFA1
172 recruitment to the focal adhesions.

173 We also looked at phosphorylation of Akt downstream of PI3K activation, which in turn is triggered
174 upon integrin activation. On treatment with CCL19, human $CD4^+$ T cells moving on ICAM-1-coated
175 plates did show a prominent leading-edge polarity of non-phosphorylated and phosphorylated Akt
176 (pAkt) (Figure 3L control panel). But in Piezo1-deficient cells the polarity of pAkt is abrogated (Figure
177 3M), not affecting the polarity of non-phosphorylated AKT (Figure 3N; Supplemental videos 7, 8),
178 substantiating the cellular signaling defect due to non-recruitment of LFA1 to the leading edge
179 membrane.

180 **Piezo1 deficiency disrupts F-actin retrograde flow in T cells despite chemokine receptor activation**

181 Piezo1-mediated sensing of membrane tension drives calcium ion influx, which in turn has been
182 shown to activate calpain and F-actin polymerization (14, 19). LFA1 recruitment is driven by local
183 actin scaffold formation following FAK assembly, which as our data indicates is perhaps contributed
184 by consolidation local actin scaffold downstream of Piezo1 activation. To confirm this, we performed
185 Ca^{2+} imaging in Piezo1-mCherry transfected Jurkat Cells using total internal reflection fluorescence
186 (TIRF) microscope in response to chemokine. We found significant colocalization of the Ca^{2+} signal
187 with the Piezo1 signal on the chemokine treated Jurkat cells (Figure 4A, B; Supplemental figure 3A,
188 B). Next to confirm that activation of calpain mediates the Piezo1 function, we observed that prior

189 inhibition with calpain inhibitor PD150606 abrogated CCL19-induced LFA1 recruitment to the leading
190 edge of the T cells. (Figure 4C, D). As expected, the upstream event of pFAK polarity was not affected
191 by the calpain inhibition (Supplemental figure 4C, D).

192 While F-actin polymerization downstream of FAK is required for LFA1 recruitment, LFA1 in turn
193 drives a more robust F-actin polymerization at the leading edge, through Akt/Rho GTPase activation.
194 Leading edge F-actin undergoes retrograde flow due to myosin contractions, thereby enabling cells
195 to move forward. We observed focal co-localization of LFA1 with F-actin at the leading edge, along
196 with a denser actin-rich protrusion in the rear edge or the uropod (Figure 4C), which was abolished
197 upon calpain inhibition (Figure 4C, E). Hence, LFA1 recruitment may depend on local F-actin
198 polarization downstream of Piezo1 activation. On the other hand, failure of LFA1 recruitment and
199 activation halts further F-actin polarization feeding the retrograde flow of actin during migration.

200 Dichotomy of Piezo1 (dense leading edge distribution) and F-actin (more dense at the rear end)
201 distribution was clearly demonstrated in cells stimulated with chemokine (Figure 4F and
202 Supplemental video 9). But, no F-actin polarity was seen on downregulating Piezo1 in the T cells
203 (Figure 4G, H; Supplemental videos 10, 11). Live cell imaging of Jurkat T cells expressing Piezo1-
204 mCherry and actin-GFP on ICAM-1 coated dishes was performed in the presence or absence of
205 SDF1α (Supplemental figure 4E). Chemokine addition showed significant increase in Piezo1 polarity
206 to the front end, as shown in the earlier experiments (Supplemental figure 4F, left). But F-actin
207 showed a dynamic balance at both ends as expected (Supplemental figure 4F, right). Polar plots
208 depicting angular distribution of Piezo1 mCherry and actin-GFP (over all time-points) in the presence
209 or absence of SDF1α are shown in Supplemental figure 3G and H. Representative image 4I and
210 supplemental video 12 shows Piezo1-mCherry distribution predominantly at the leading edge and
211 actin-GFP eventually accumulating at the rear end in uropod-like cellular extensions in a migrating
212 Jurkat T cell.

213 Thus, our data reveals a membrane-intrinsic event, involving a critical role of Piezo1
214 mechanosensors, within the outside-in signaling module in response to chemokine receptor
215 activation in human T cells. The mechanistic model derived from our data is depicted in Figure 4J.
216 The Piezo1 mechanosensing links the focal adhesion assembly to integrins recruitment at the leading
217 edge of the human T cells migrating in response to chemokine activation and thus play a critical role
218 in chemotactic migration of human T cells.

219

220 **DISCUSSION**

221 The present study explored the role of membrane-intrinsic tension generation and the crucial role of
222 sensing this physical cue in the context of human T cell migration in response to chemokine receptor
223 activation. Deficiency of Piezo1 inhibited integrin-dependent migration, demonstrating crucial role
224 of these mechanosensors in this mode of T cell migration. As the integrin-dependent chemotactic
225 migration of T cells is a critically implicated in most patho-physiologic contexts, in the present study
226 we focused on the potential role of Piezo1 mechanosensors in this specific context.

227 Notably, a previous study in vivo in mice, using genetic deletion of Piezo1 in T cells, reported no
228 significant effect on tissue recruitment of T cells (17). Although a functional redundancy in the role
229 of Piezo1-mediated mechanosensing in mouse T cells warrants exclusion, especially in case of gene
230 deletion in developing T cells, given the considerable expression of Piezo2 as well in mouse T cells
231 (39). On the other hand, a role of Piezo1 activation in fibroblastic reticular cells in Peyer's patches
232 has been shown to regulate lymphocyte migration through tissue conduits (40). The different tissue
233 distribution of Piezo1 and Piezo2 expression in humans warranted exploring the role of Piezo1 in
234 migrating human T cells, as in humans Piezo2 is hardly expressed in the hematopoietic cells.

235 Non-invasive interference reflection microscopy allowed us to demonstrate dynamic change in
236 membrane tension at the leading edge of T cells stimulated with chemokine on ICAM1-bed which
237 was closely followed by dynamic recruitment Piezo1 locally. Chemokine receptor activation leads to
238 focal adhesion formation at the leading edge of the migrating T cells (33, 34). Our experiments
239 revealed that Piezo1 recruitment at the leading edge of the cells followed focal adhesion kinase
240 activation. Focal adhesions do increase local membrane tension as they connect the extracellular
241 environment with the cortical cytoskeleton of the cell (33). Piezo1 recruitment locally seems to be a
242 response to this membrane tension increase at focal adhesions.

243 'Outside-in' signaling downstream of focal adhesion formation recruits integrins to the leading edge
244 of the moving T cells (35, 36) which was abrogated by Piezo1 downregulation. Piezo1 has been
245 shown to drive Ca^{2+} influx into the T cells leading to calpain activation (14, 19). As expected, calpain
246 inhibition also interfered with leading edge recruitment of the integrin LFA-1. Plausibly calpain
247 activation drives local F-actin polymerization at the leading edge facilitating LFA-1 recruitment. This
248 was also supported by loss of polarity of AKT phosphorylation with Piezo1 deficiency, which is known
249 to be the major downstream signaling module that succeeds LFA-1 recruitment and activation (38,
250 41). These dysregulations in turn abrogates the retrograde flow of actin in the moving cell that is
251 essential for forward propulsion of the cell body (6, 7, 37, 41). Of note here, a role of ER-resident
252 Piezo1, in driving R-RAS-driven activation of integrins, which was again dependent on calpain
253 activation, was reported even before the mechanosensing function of Piezo1 was established (30).

254 Thus, the present study reports a hitherto unexplored role of the professional mechanosensor
255 Piezo1 in integrin dependent chemotactic movement of human T cells. In the cascade of leading
256 edge events in a moving human T cell, following chemokine receptor activation and eventually
257 leading to the retrograde flow of actin, focal adhesion formation precedes Piezo1 activation, while
258 LFA-1 recruitment is dependent on Piezo1 function.

259

260 **ACKNOWLEDGEMENTS**

261 The study was funded by Council of Scientific and Industrial Research, India (Grant no. FBR MLP-
262 140). D.G. is a recipient of Swarnajayanti Fellowship from Department of Science and Technology,
263 Government of India. The authors express their gratitude for provision of the Piezo1 constructs by
264 Dr. Charles Cox, Victor Chang Institute of Cardiac Research, Australia.

265 The authors declare no competing interests

266 C.S.C.L. designed, performed and analyzed most of the experiments, prepared the figures and took
267 part in writing the manuscript; T.M., B.S. and C.S.C.L. performed the IRM experiments; T.M. and B.S.
268 analyzed IRM data; C.S.C.L., P.B. and D.K.S. performed image analyses; Pu.B., M.A.H., B.P.S., J.S. and
269 R.D. helped with cell culture and confocal microscopy experiments; D.G. conceptualized and
270 supervised the study, acquired funding, designed experiments and wrote the manuscript with input
271 from all authors.

272

273 **REFERENCES**

274 1. Shechter R, London A, Schwartz M. Orchestrated leukocyte recruitment to immune-
275 privileged sites: absolute barriers versus educational gates. Nat Rev Immunol. 2013
276 Mar;13(3):206-18. doi: 10.1038/nri3391.
277 2. Krummel MF, Bartumeus F, Gérard A. T cell migration, search strategies and mechanisms.
278 Nat Rev Immunol. 2016 Mar;16(3):193-201. doi: 10.1038/nri.2015.16.
279 3. Woodland DL, Kohlmeier JE. Migration, maintenance and recall of memory T cells in
280 peripheral tissues. Nat Rev Immunol. 2009 Mar;9(3):153-61. doi: 10.1038/nri2496.
281 4. Masopust D, Schenkel JM. The integration of T cell migration, differentiation and function.
282 Nat Rev Immunol. 2013 May;13(5):309-20. doi: 10.1038/nri3442.
283 5. Fowell DJ, Kim M. The spatio-temporal control of effector T cell migration. Nat Rev Immunol.
284 2021 Sep;21(9):582-596. doi: 10.1038/s41577-021-00507-0.

285 6. Dupré L, Houmadi R, Tang C, Rey-Barroso J. T Lymphocyte Migration: An Action Movie
286 Starring the Actin and Associated Actors. Front Immunol. 2015 Nov 18;6:586. doi:
287 10.3389/fimmu.2015.00586.
288 7. Nordenfelt P, Moore TI, Mehta SB, Kalappurakkal JM, Swaminathan V, Koga N, Lambert TJ,
289 Baker D, Waters JC, Oldenbourg R, Tani T, Mayor S, Waterman CM, Springer TA. Direction of
290 actin flow dictates integrin LFA-1 orientation during leukocyte migration. Nat Commun. 2017
291 Dec 11;8(1):2047. doi: 10.1038/s41467-017-01848-y.
292 8. Moreau HD, Piel M, Voituriez R, Lennon-Duménil AM. Integrating Physical and Molecular
293 Insights on Immune Cell Migration. Trends Immunol. 2018 Aug;39(8):632-643. doi:
294 10.1016/j.it.2018.04.007.
295 9. Shannon MJ, Pineau J, Griffié J, Aaron J, Peel T, Williamson DJ, Zamoyska R, Cope AP, Cornish
296 GH, Owen DM. Differential nanoscale organisation of LFA-1 modulates T-cell migration. J Cell
297 Sci. 2019 Oct 16;133(5):jcs232991. doi: 10.1242/jcs.232991.
298 10. Coste B, Mathur J, Schmidt M, Earley TJ, Ranade S, Petrus MJ, Dubin AE, Patapoutian A.
299 Piezo1 and Piezo2 are essential components of distinct mechanically activated cation
300 channels. Science. 2010 Oct 1;330(6000):55-60. doi: 10.1126/science.1193270.
301 11. Coste B, Xiao B, Santos JS, Syeda R, Grandl J, Spencer KS, Kim SE, Schmidt M, Mathur J, Dubin
302 AE, Montal M, Patapoutian A. Piezo proteins are pore-forming subunits of mechanically
303 activated channels. Nature. 2012 Feb 19;483(7388):176-81. doi: 10.1038/nature10812.
304 12. Syeda R, Florendo MN, Cox CD, Kefauver JM, Santos JS, Martinac B, Patapoutian A. Piezo1
305 Channels Are Inherently Mechanosensitive. Cell Rep. 2016 Nov 8;17(7):1739-1746. doi:
306 10.1016/j.celrep.2016.10.033.
307 13. Murthy SE, Dubin AE, Patapoutian A. Piezos thrive under pressure: mechanically activated
308 ion channels in health and disease. Nat Rev Mol Cell Biol. 2017 Dec;18(12):771-783. doi:
309 10.1038/nrm.2017.92. Epub 2017 Oct 4. PMID: 28974772.
310 14. Liu CSC, Raychaudhuri D, Paul B, Chakrabarty Y, Ghosh AR, Rahaman O, Talukdar A, Ganguly
311 D. Cutting Edge: Piezo1 Mechanosensors Optimize Human T Cell Activation. J Immunol. 2018
312 Feb 15;200(4):1255-1260. doi: 10.4049/jimmunol.1701118.
313 15. Atcha H, Jairaman A, Holt JR, Meli VS, Nagalla RR, Veerasubramanian PK, Brumm KT, Lim HE,
314 Othy S, Cahalan MD, Pathak MM, Liu WF. Mechanically activated ion channel Piezo1
315 modulates macrophage polarization and stiffness sensing. Nat Commun. 2021 May
316 31;12(1):3256. doi: 10.1038/s41467-021-23482-5.
317 16. Geng J, Shi Y, Zhang J, Yang B, Wang P, Yuan W, Zhao H, Li J, Qin F, Hong L, Xie C, Deng X, Sun
318 Y, Wu C, Chen L, Zhou D. TLR4 signalling via Piezo1 engages and enhances the macrophage

319 mediated host response during bacterial infection. Nat Commun. 2021 Jun 10;12(1):3519.
320 doi: 10.1038/s41467-021-23683-y.
321 17. Jairaman A, Othy S, Dynes JL, Yeromin AV, Zavala A, Greenberg ML, Nourse JL, Holt JR,
322 Cahalan SM, Marangoni F, Parker I, Pathak MM, Cahalan MD. Piezo1 channels restrain
323 regulatory T cells but are dispensable for effector CD4+ T cell responses. Sci Adv. 2021 Jul
324 7;7(28):eabg5859. doi: 10.1126/sciadv.abg5859.
325 **18.** Jäntti H, Sitnikova V, Ishchenko Y, Shakirzyanova A, Giudice L, Ugidos IF, Gómez-Budia M,
326 Korvenlaita N, Ohtonen S, Belaya I, Fazaludeen F, Mikhailov N, Gotkiewicz M, Ketola K,
327 Lehtonen Š, Koistinaho J, Kanninen KM, Hernández D, Pébay A, Giugno R, Korhonen P,
328 Giniatullin R, Malm T. Microglial amyloid beta clearance is driven by PIEZO1 channels. J
329 Neuroinflammation. 2022 Jun 15;19(1):147. doi: 10.1186/s12974-022-02486-y.
330 19. Liu CSC, Ganguly D. Mechanical Cues for T Cell Activation: Role of Piezo1 Mechanosensors.
331 Crit Rev Immunol. 2019;39(1):15-38. doi: 10.1615/CritRevImmunol.2019029595.
332 20. Ma S, Dubin AE, Zhang Y, Mousavi SAR, Wang Y, Coombs AM, Loud M, Andolfo I,
333 Patapoutian A. A role of PIEZO1 in iron metabolism in mice and humans. Cell. 2021 Feb
334 18;184(4):969-982.e13. doi: 10.1016/j.cell.2021.01.024.
335 21. He Y, Deng B, Liu S, Luo S, Ning Y, Pan X, Wan R, Chen Y, Zhang Z, Jiang J, Xu H, Xia M, Li J.
336 Myeloid Piezo1 Deletion Protects Renal Fibrosis by Restraining Macrophage Infiltration and
337 Activation. Hypertension. 2022 May;79(5):918-931. doi:
338 10.1161/HYPERTENSIONAHA.121.18750.
339 22. Huang Z, Sun Z, Zhang X, Niu K, Wang Y, Zheng J, Li H, Liu Y. Loss of stretch-activated
340 channels, PIEZOs, accelerates non-small cell lung cancer progression and cell migration.
341 Biosci Rep. 2019 Mar 22;39(3): BSR20181679. doi: 10.1042/BSR20181679.
342 23. Chubinskiy-Nadezhdin VI, Vasileva VY, Vassilieva IO, Sudarikova AV, Morachevskaya EA,
343 Negulyaev YA. Agonist-induced Piezo1 activation suppresses migration of transformed
344 fibroblasts. Biochem Biophys Res Commun. 2019 Jun 18;514(1):173-179. doi:
345 10.1016/j.bbrc.2019.04.139.
346 24. Mousawi F, Peng H, Li J, Ponnambalam S, Roger S, Zhao H, Yang X, Jiang LH. Chemical
347 activation of the Piezo1 channel drives mesenchymal stem cell migration via inducing ATP
348 release and activation of P2 receptor purinergic signaling. Stem Cells. 2020 Mar;38(3):410-
349 421. doi: 10.1002/stem.3114.
350 25. Wang X, Cheng G, Miao Y, Qiu F, Bai L, Gao Z, Huang Y, Dong L, Niu X, Wang X, Li Y, Tang H,
351 Xu Y, Song X. Piezo type mechanosensitive ion channel component 1 facilitates gastric

352 cancer omentum metastasis. J Cell Mol Med. 2021 Feb;25(4):2238-2253. doi:
353 10.1111/jcmm.16217.
354 26. Gao L, Ji Y, Wang L, He M, Yang X, Qiu Y, Sun X, Ji Z, Yang G, Zhang J, Li S, Dai L, Zhang L.
355 Suppression of Esophageal Squamous Cell Carcinoma Development by Mechanosensitive
356 Protein Piezo1 Downregulation. ACS Omega. 2021 Apr 12;6(15):10196-10206. doi:
357 10.1021/acsomega.1c00505.
358 27. Holt JR, Zeng WZ, Evans EL, Woo SH, Ma S, Abuwarda H, Loud M, Patapoutian A, Pathak MM.
359 Spatiotemporal dynamics of PIEZO1 localization controls keratinocyte migration during
360 wound healing. Elife. 2021 Sep 27;10:e65415. doi: 10.7554/eLife.65415.
361 28. Velasco-Estevez M, Koch N, Klejbor I, Caratis F, Rutkowska A. Mechanoreceptor Piezo1 Is
362 Downregulated in Multiple Sclerosis Brain and Is Involved in the Maturation and Migration
363 of Oligodendrocytes in vitro. Front Cell Neurosci. 2022 May 26;16:914985. doi:
364 10.3389/fncel.2022.914985.
365 29. Hung WC, Yang JR, Yankaskas CL, Wong BS, Wu PH, Pardo-Pastor C, Serra SA, Chiang MJ, Gu
366 Z, Wirtz D, Valverde MA, Yang JT, Zhang J, Konstantopoulos K. Confinement Sensing and
367 Signal Optimization via Piezo1/PKA and Myosin II Pathways. Cell Rep. 2016 May
368 17;15(7):1430-1441. doi: 10.1016/j.celrep.2016.04.035.
369 30. McHugh BJ, Buttery R, Lad Y, Banks S, Haslett C, Sethi T. Integrin activation by Fam38A uses a
370 novel mechanism of R-Ras targeting to the endoplasmic reticulum. J Cell Sci. 2010 Jan
371 1;123(Pt 1):51-61. doi: 10.1242/jcs.056424.
372 31. Barr VA, Bunnell SC. Interference reflection microscopy. Curr Protoc Cell Biol. 2009 Dec;
373 Chapter 4: Unit 4.23. doi: 10.1002/0471143030.cb0423s45.
374 32. Chakraborty M, Mukherjee B, Nalinakshan N, Biswas A, Nayak RK, Sinha B. Effect of
375 heterogeneous substrate adhesivity of follower cells on speed and tension profile of leader
376 cells in primary keratocyte collective cell migration. Biol Open. 2022 Mar
377 15;11(3):bio058893. doi: 10.1242/bio.058893.
378 33. Mitra SK, Hanson DA, Schlaepfer DD. Focal adhesion kinase: in command and control of cell
379 motility. Nat Rev Mol Cell Biol. 2005 Jan;6(1):56-68. doi: 10.1038/nrm1549.
380 34. Katoh K. FAK-Dependent Cell Motility and Cell Elongation. Cells. 2020 Jan 12;9(1):192. doi:
381 10.3390/cells9010192.
382 35. Yamashiro S, Watanabe N. A new link between the retrograde actin flow and focal
383 adhesions. J Biochem. 2014 Nov;156(5):239-48. doi: 10.1093/jb/mvu053.
384 36. Martino F, Perestrelo AR, Vinarský V, Pagliari S, Forte G. Cellular Mechanotransduction:
385 From Tension to Function. Front Physiol. 2018 Jul 5;9:824. doi: 10.3389/fphys.2018.00824.

386 37. Sánchez-Martín L, Sánchez-Sánchez N, Gutiérrez-López MD, Rojo AI, Vicente-Manzanares M,
387 Pérez-Alvarez MJ, Sánchez-Mateos P, Bustelo XR, Cuadrado A, Sánchez-Madrid F, Rodríguez-
388 Fernández JL, Cabañas C. Signaling through the leukocyte integrin LFA-1 in T cells induces a
389 transient activation of Rac-1 that is regulated by Vav and PI3K/Akt-1. J Biol Chem. 2004 Apr
390 16;279(16):16194-205. doi: 10.1074/jbc.M400905200.
391 38. Roy NH, Kim SHJ, Buffone A Jr, Blumenthal D, Huang B, Agarwal S, Schwartzberg PL, Hammer
392 DA, Burkhardt JK. LFA-1 signals to promote actin polymerization and upstream migration in T
393 cells. J Cell Sci. 2020 Sep 9;133(17):jcs248328. doi: 10.1242/jcs.248328.
394 39. Ganguly D. Can Piezo2 substitute Piezo1 function in the context of T cell-specific deletion in
395 mice? Sci Adv, e-Letter published Sep 8, 2021, in response to Jairaman A et al.,
396 40. Chang JE, Buechler MB, Gressier E, Turley SJ, Carroll MC. Mechanosensing by Peyer's patch
397 stroma regulates lymphocyte migration and mucosal antibody responses. Nat Immunol.
398 2019 Nov;20(11):1506-1516. doi: 10.1038/s41590-019-0505-z.
399 41. Roy NH, MacKay JL, Robertson TF, Hammer DA, Burkhardt JK. Crk adaptor proteins mediate
400 actin-dependent T cell migration and mechanosensing induced by the integrin LFA-1. Sci
401 Signal. 2018 Dec 11;11(560):eaat3178. doi: 10.1126/scisignal.aat3178.
402 42. Limozin L, Sengupta K. Quantitative reflection interference contrast microscopy (RICM) in
403 soft matter and cell adhesion. Chemphyschem. 2009 Nov 9;10(16):2752-68.
404 43. Biswas A, Alex A, Sinha B. Mapping Cell Membrane Fluctuations Reveals Their Active
405 Regulation and Transient Heterogeneities. Biophys J. 2017 Oct 17;113(8):1768-1781. doi:
406 10.1016/j.bpj.2017.08.041.
407 44. Biswas A, Kashyap P, Datta S, Sengupta T, Sinha B. Cholesterol Depletion by MβCD Enhances
408 Cell Membrane Tension and Its Variations-Reducing Integrity. Biophys J. 2019 Apr
409 23;116(8):1456-1468.
410 45. Shiba H, Noguchi H, Fournier JB. Monte Carlo study of the frame, fluctuation and internal
411 tensions of fluctuating membranes with fixed area. Soft Matter. 2016 Feb 28;12(8):2373-80.
412 doi: 10.1039/c5sm01900a.

413 **FIGURE LEGENDS**

414 **Figure 1. Piezo1 deficiency abrogates integrin-dependent motility in human T cells which is**
415 **mediated through redistribution of Piezo1 at the leading edge in response to chemokine**
416 **stimulation.**

417 **A.** MSD versus time calculated for GFP^+ (potential Piezo1-knockdown cells) and GFP^- (potential
418 control cells) in GFP plasmid and Piezo1 siRNA co-transfected human $CD4^+$ T lymphocytes, that were
419 allowed to migrate in presence of recombinant CCL19 on ICAM1-coated dishes. **B.** Representative
420 tracks of GFP^+ and GFP^- $CD4^+$ T lymphocytes. Comparisons of **C.** % GFP^+ cells after 72 hours of
421 nucleofection **D & E.** 3D transwell migration assay of siRNA-transfected primary human $CD4^+$ T
422 lymphocytes (D) and Jurkat T cells (E), respectively. Data representative of at least 3 independent
423 experiments. **F.** Representative confocal images of Piezo1 distribution in fixed untreated and CCL19-
424 treated $CD4^+$ T lymphocytes. 63X oil magnification. **G.** Comparison between Piezo1 polarity index
425 calculated for fixed, stained, human $CD4^+$ T lymphocytes with or without 0.5µg/ml CCL19 treatment
426 for 20-30 minutes. n > 510 random cells, each. **H.** Piezo1 polarity index calculated for Jurkat cells,
427 expressing mCherry-tagged Piezo1 during live-cell tracking in the presence of recombinant SDF1α.
428 Each dot represents polarity index of each cell, averaged over all the time-frames. **I.** Representative
429 time kinetics of particle image velocimetry (PIV) analysis of Piezo1-mcherry transfected Jurkat cells,
430 allowed to move on ICAM-coated dishes in the presence of recombinant SDF1α. Top panel: No
431 chemokine. Bottom Panel: SDF1α.

432

433 **Figure 2. Piezo1 redistribution in migrating T cells follow increased membrane tension in the**
434 **leading edge**

435 **A.** Schematic illustration of interference reflection microscopy imaging setup. **B.** Probability
436 distribution of amplitude of temporal fluctuations (SD_{time}, left) and tension (right) before and after
437 addition of chemokines. **C.** Temporal trajectory of tension of cells before and after addition of
438 chemokine with ** indicating significant difference from control. **D.** Representative IRM images of
439 Jurkat cells (top), corresponding tension maps (middle) and R^2 maps (bottom), before and after
440 chemokine treatment. **E** Correlation between normalized Piezo intensity, tension magnitudes with
441 time. **F.** Scatter plot to show correlation between normalized pixel count of Piezo1 and normalized
442 tension. Piezo1 intensity at specific time-points were correlated with tension magnitudes at the
443 preceding timepoints. Normalization has been done such that the maximum value is set to 1 and
444 others are accordingly scaled. **G.** Colour-coded Piezo1-GFP intensity map (left), epifluorescence

445 image (middle), and tension map (right) of representative Piezo1-GFP expressing Jurkat cell, after 30
446 minutes of 0.1μg/ml of SDF1α treatment.

447

448 **Figure 3. Focal adhesion following chemokine receptor activation does not depend on Piezo1 while**
449 **membrane recruitment of LFA1 on chemokine receptor activation disrupts with Piezo1 deficiency.**

450 **A.** Representative confocal images of human $CD4^+$ T lymphocytes, fixed and stained for phospho-FAK
451 (pFAK) under untreated and CCL19-treated conditions. **B.** Increased polarity of pFAK upon
452 chemokine stimulation of $CD4^+$ T lymphocytes as compared to unstimulated controls. N > 120 cells,
453 each. **C.** Representative confocal images of pFAK distribution in control and Piezo1 siRNA-transfected
454 $CD4^+$ T lymphocytes stimulated with chemokine. **D**. Comparison of pFAK polarity in CCL19-stimulated
455 control and Piezo1-knockdown $CD4^+$ T lymphocytes. n > 450 random cells, each. **E.** Representative
456 confocal images of stained Piezo1 in $CD4^+$ T cells stimulated with CCL19 in the presence or absence
457 of FAK inhibitor 14. **F.** Effect of FAK inhibition on Piezo1 polarity in $CD4^+$ T lymphocytes stimulated
458 with recombinant CCL19 versus untreated cells. n > 600 random cells, each. Data represented from
459 at least 3 independent experiments. **G.** Representative confocal images of fixed, immunostained
460 Piezo1 and LFA1 in unstimulated and CCL19-stimulated $CD4^+$ T lymphocytes. **H.** Increased LFA1
461 polarity in response to recombinant CCL19 stimulation in $CD4^+$ T cells. n > 295 random cells, each. **I.**
462 Manders' co-localisation analysis of Piezo1 and LFA1 in untreated and CCL19-treated $CD4^+$ T
463 lymphocytes. **J.** Comparison of LFA1 polarity in chemokine-treated control and Piezo1 knockdown
464 $CD4^+$ T lymphocytes. **K.** Representative confocal stained images of LFA1 polarity of CCL19-treated
465 control and Piezo1-knockdown $CD4^+$ T lymphocytes. n > 490 random cells, each. **L.** Representative
466 confocal images of phospho-Akt (pAkt) and Akt distribution upon chemokine treatment of control
467 and Piezo1-knockdown cells. **M & N.** Quantitative analyses of pAkt (M) and Akt (N) polarity in control
468 and Piezo1-knockdown cells after CCL19-treatment. n > 580 random cells, each. Data represented
469 from at least 3 independent experiments.

470

471 **Figure 4. Piezo1 deficiency disrupts F-actin retrograde flow in T cells despite chemokine receptor**
472 **activation.**

473 **A.** Representative TIRF image of a Jurkat cell stained with Fluo-3 AM and expressing Piezo1 mCherry.
474 Lower panel: zoomed in image and overlap of binary images of objects detected from Ca^{2+} and
475 Piezo1 signals as well as simulated randomly placed puncta having similar total (in the zoomed in
476 section) and average area as that of the Ca^{2+} puncta detected in the real images. Overlap RGB image

477 shows the overlap between Real Ca^{2+} puncta (red) and Piezo1 puncta (green), overlap puncta
478 (yellow), simulated Ca^{2+} puncta (blue). **B.** Comparison between percentage Ca^{2+} colocalization of
479 simulated data and real data. * denotes *p*-value < 0.05 calculated using Mann Whitney U test. N_{cell}=
480 52 (13 cells x 4 time points). N_{ROIS}= 52. **C.** Representative confocal images of LFA1 and actin
481 distribution in CCL19-stimulated $CD4^+$ T lymphocytes with or without inhibition of calpain.
482 Quantitative comparisons of **D.** LFA1 and **E.** actin polarity upon chemokine stimulation, in the
483 presence or absence of calpain pre-inhibition. N > 290 random cells, each. **F.** Representative fixed
484 confocal images of actin and Piezo1 distribution in $CD4^+$ T lymphocytes after 30 mins of 0.5µg/ml
485 recombinant CCL19 treatment. **G.** Quantitative comparison of actin polarity in control and Piezo1-
486 knockdown $CD4^+$ T lymphocytes cells after 30 mins of chemokine treatment. n > 300 random cells,
487 each. **H.** Representative fixed confocal images of actin distribution in chemokine-treated, control
488 and Piezo1-knockdown $CD4^+$ T lymphocytes. **I.** A snapshot of time-lapse imaging of Piezo1-mCherry
489 and actin-GFP expressing Jurkat cell treated with 0.1µg/ml of SDF1α. Image is maximum Z-projection
490 of the cell at 63X/1.40 magnification. **J.** Proposed model suggests chemokine receptor activation in
491 human T cells lead to focal adhesion kinase activation and focal adhesion formation. Focal adhesions
492 lead to localized increase in membrane tension at the leading edge plasma membrane which leads
493 to Piezo1 recruitment and activation. Piezo1 activation leads to calpain activation which potentially
494 drives further cytoskeletal consolidation to recruit integrin LFA1. LFA1 recruitment and activation
495 lead to phosphorylation of AKT and downstream signaling eventually driving the retrograde actin
496 flow in migrating human T cells.

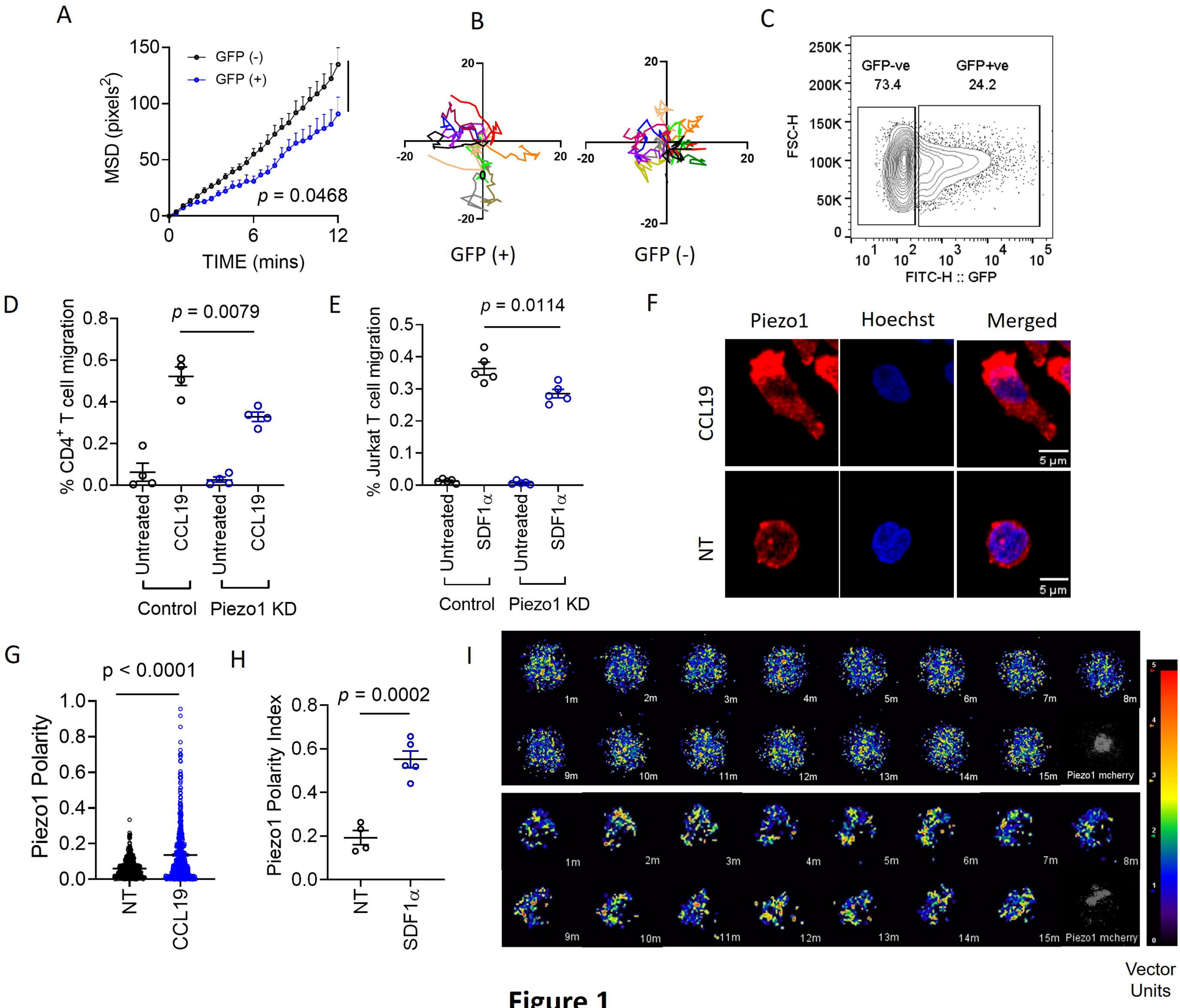
A
MSD (pixels²)
GFP (-)
GFP (+)
p = 0.0468
TIME (mins)
B
GFP (+)
GFP (-)
C
GFP-ve
73.4
GFP+ve
24.2
FSC-H
FITC-H :: GFP
D
% CD4⁺ T cell migration
p = 0.0079
Untreated
CCL19
Control
Piezo1 KD
E
% Jurkat T cell migration
p = 0.0114
Untreated
SDF1α
Control
Piezo1 KD
F
Piezo1
Hoechst
Merged
CCL19
NT
5 µm
G
Piezo1 Polarity
p < 0.0001
NT
CCL19
H
Piezo1 Polarity Index
p = 0.0002
NT
SDF1α
I
1m
2m
3m
4m
5m
6m
7m
8m
9m
10m
11m
12m
13m
14m
15m
Piezo1 mcherry
Vector Units

Figure 1

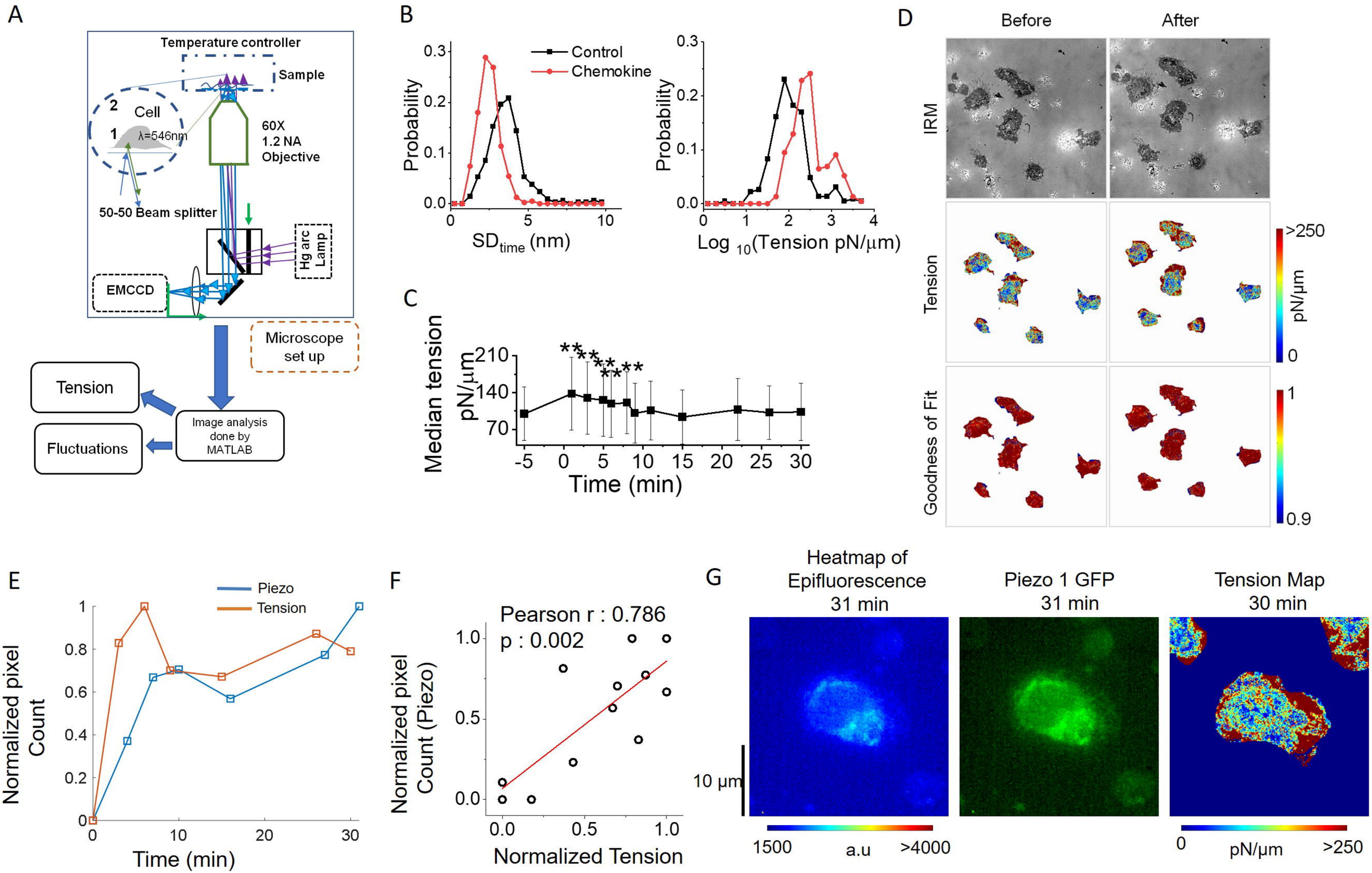
A
Temperature controller
Sample
Cell
2
1
λ=546nm
60X
1.2 NA
Objective
50-50 Beam splitter
Hg arc Lamp
EMCCD
Microscope set up
Tension
Fluctuations
Image analysis done by MATLAB
B
Control
Chemokine
Probability
SD time (nm)
Log 10(Tension pN/μm)
C
Median tension pN/μm
Time (min)
D
Before
After
IRM
Tension
Goodness of Fit
>250
pN/μm
0
1
0.9
E
Piezo
Tension
Normalized pixel Count
Time (min)
F
Pearson r : 0.786
p : 0.002
Normalized pixel Count (Piezo)
Normalized Tension
G
Heatmap of Epifluorescence 31 min
Piezo 1 GFP 31 min
Tension Map 30 min
10 μm
1500
a.u
>4000
0
pN/μm
>250

Figure 2

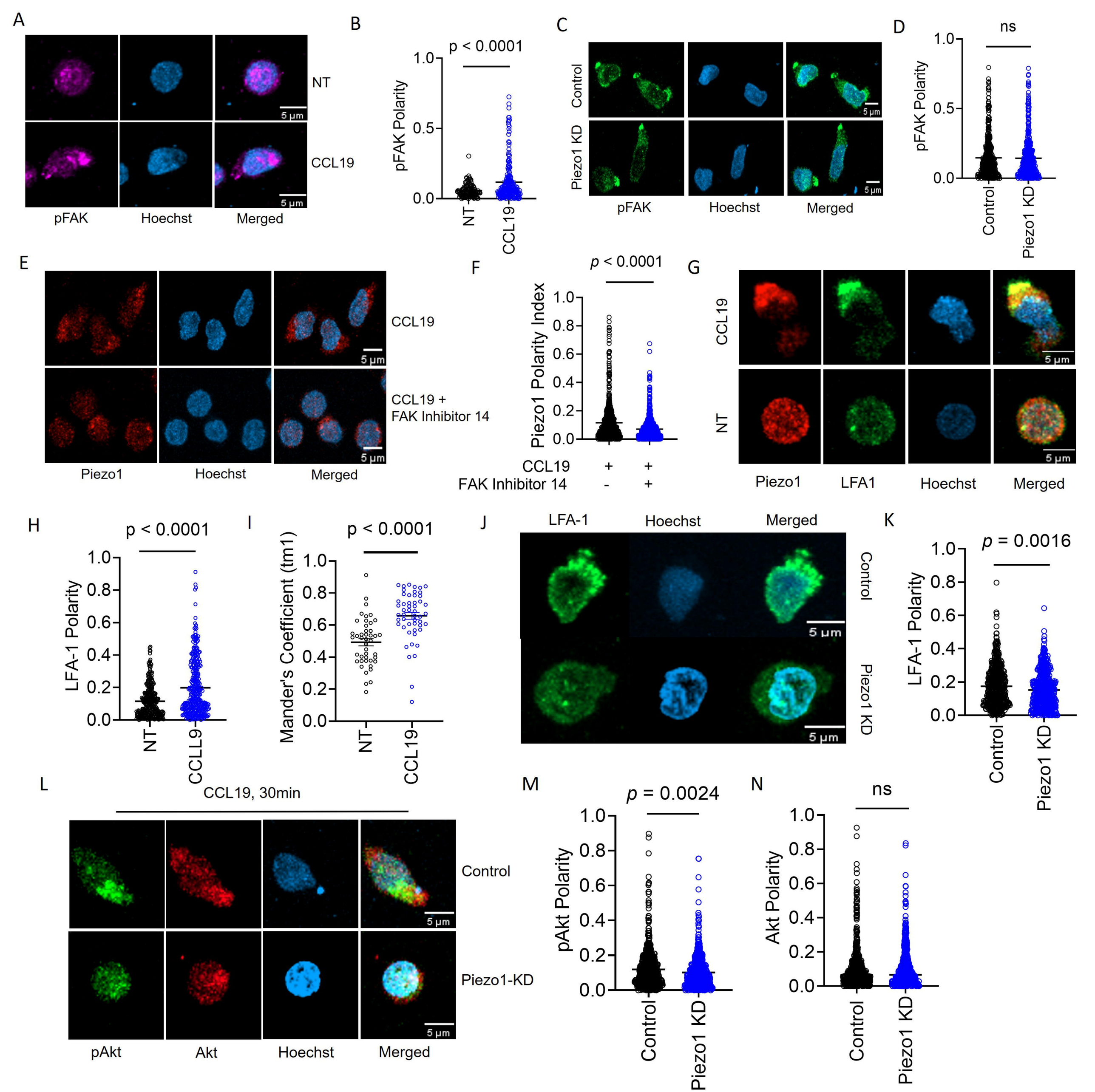
A
NT
CCL19
5 µm
pFAK
Hoechst
Merged
B
p < 0.0001
pFAK Polarity
1.0
0.5
0.0
NT
CCL19
C
Control
Piezo1 KD
pFAK
Hoechst
Merged
D
ns
pFAK Polarity
Control
Piezo1 KD
E
CCL19
CCL19 +
FAK Inhibitor 14
Piezo1
Hoechst
Merged
F
p < 0.0001
Piezo1 Polarity Index
CCL19 + +
FAK Inhibitor 14 - +
G
CCL19
NT
Piezo1
LFA1
Hoechst
Merged
H
p < 0.0001
LFA-1 Polarity
NT
CCLL9
I
p < 0.0001
Mander's Coefficient (tm1)
NT
CCL19
J
LFA-1
Hoechst
Merged
Control
Piezo1 KD
K
p = 0.0016
LFA-1 Polarity
Control
Piezo1 KD
L
CCL19, 30min
Control
Piezo1-KD
pAkt
Akt
Hoechst
Merged
M
p = 0.0024
pAkt Polarity
Control
Piezo1 KD
N
ns
Akt Polarity
Control
Piezo1 KD

Figure 3

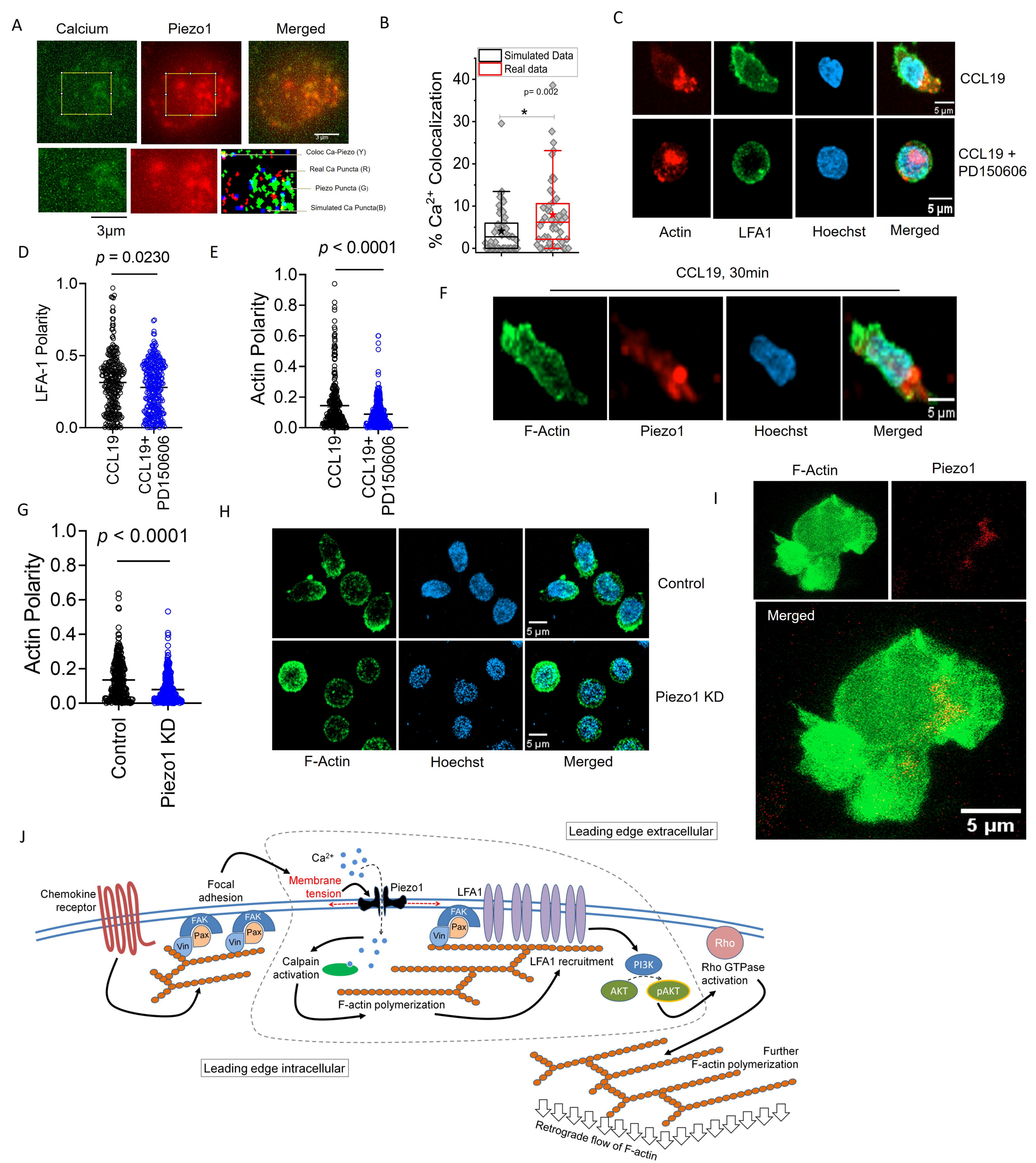
A
Calcium
Piezo1
Merged
3 µm
Coloc Ca-Piezo (Y)
Real Ca Puncta (R)
Piezo Puncta (G)
Simulated Ca Puncta(B)
3µm
B
Simulated Data
Real data
p= 0.002
% Ca2+ Colocalization
C
CCL19
CCL19 + PD150606
5 µm
Actin
LFA1
Hoechst
Merged
D
p = 0.0230
LFA-1 Polarity
CCL19
CCL19+ PD150606
E
p < 0.0001
Actin Polarity
F
CCL19, 30min
F-Actin
Piezo1
Hoechst
Merged
G
p < 0.0001
Actin Polarity
Control
Piezo1 KD
H
Control
Piezo1 KD
F-Actin
Hoechst
Merged
I
F-Actin
Piezo1
Merged
5 µm
J
Leading edge extracellular
Leading edge intracellular
Chemokine receptor
Focal adhesion
Membrane tension
Ca2+
Piezo1
LFA1
FAK
Pax
Vin
Calpain activation
LFA1 recruitment
F-actin polymerization
PI3K
AKT
pAKT
Rho
Rho GTPase activation
Further F-actin polymerization
Retrograde flow of F-actin

Figure 4